THE JOURNAL OF IMMUNOLOGY

Induction of Functional Human Macrophages from Bone Marrow Promonocytes by M-CSF in Humanized Mice

Yan Li, Qingfeng Chen, Dahai Zheng, Lu Yin, Yok Hian Chionh, Lan Hiong Wong, Shu Qi Tan, Thiam Chye Tan, Jerry K. Y. Chan, Sylvie Alonso, Peter C. Dedon, Bing Lim and Jianzhu Chen

J Immunol 2013; 191:3192-3199; Prepublished online 9 August 2013;
doi: 10.4049/jimmunol.1300742
http://www.jimmunol.org/content/191/6/3192

The Journal of Immunology is published twice each month by
The American Association of Immunologists, Inc.,
9650 Rockville Pike, Bethesda, MD 20814-3994.

Print ISSN: 0022-1767 Online ISSN: 1550-6606.

Induction of Functional Human Macrophages from Bone Marrow Promonocytes by M-CSF in Humanized Mice

Yan Li,*,[1] Qingfeng Chen,*,†,‡,[1] Dahai Zheng,* Lu Yin,* Yok Hian Chionh,* Lan Hiong Wong,* Shu Qi Tan,[§] Thiam Chye Tan,[§,¶] Jerry K. Y. Chan,[‖,#,] Sylvie Alonso,*,‡ Peter C. Dedon,*,†† Bing Lim,‡‡ and Jianzhu Chen*,§§**

Engraftment of human CD34$^+$ hematopoietic stem/progenitor cells into immunodeficient mice leads to robust reconstitution of human T and B cells but not monocytes and macrophages. To identify the cause underlying the poor monocyte and macrophage reconstitution, we analyzed human myeloid cell development in humanized mice and found that it was blocked at the promonocyte stage in the bone marrow. Expression of human M-CSF or GM-CSF by hydrodynamic injection of cytokine-encoding plasmid completely abolished the accumulation of promonocytes in the bone marrow. M-CSF promoted the development of mature monocytes and tissue-resident macrophages whereas GM-CSF did not. Moreover, correlating with an increased human macrophages at the sites of infection, M-CSF–treated humanized mice exhibited an enhanced protection against influenza virus and *Mycobacterium* infection. Our study identifies the precise stage at which human monocyte/macrophage development is blocked in humanized mice and reveals overlapping and distinct functions of M-CSF and GM-CSF in human monocyte and macrophage development. The improved reconstitution and functionality of monocytes/macrophages in the humanized mice following M-CSF expression provide a superior in vivo system to investigate the role of macrophages in physiological and pathological processes.
***The Journal of Immunology*, 2013, 191: 3192–3199.**

Macrophages, monocytes, and dendritic cells (DC) form the mononuclear phagocytic system. These phagocytic cells are derived from the common myeloid precursors in the bone marrow (BM). In the periphery, monocytes circulate in the blood, whereas macrophages and DCs reside in the tissues. Development of monocytes and macrophages is controlled by cytokines, including M-CSF (also known as CSF-1), GM-CSF, and IL-34. M-CSF was originally identified by its ability to stimulate the generation of macrophage colonies when added to cultures of BM progenitor cells in vitro (1). CSF1^{op}/CSF1^{op} mice, which produce an aberrant form of M-CSF, exhibit a severely reduced cellularity in the BM, a reduced number of circulating monocytes and deficiency in some tissue macrophage populations (2–5). However, follow-up studies showed that there is no reduction in circulating monocytes, and the selective deficiency in tissue macrophage populations is corrected as CSF1^{op}/CSF1^{op} mice age (6, 7). Because of the conflicting results, whether M-CSF functions in monocyte production in the BM or at the transition of monocyte into macrophage in the tissues is still controversial (3, 4, 6, 8–10). GM-CSF was identified to stimulate the generation of granulocyte and macrophage colonies when added to the BM cell culture in vitro. Unlike M-CSF, deficiency in GM-CSF does not compromise the steady state of myelopoiesis and production of tissue macrophages, except the maturation of alveolar macrophages in the lungs (11). Recently, IL-34 was found to bind to M-CSF receptor and exhibited similar functions as M-CSF in promoting the formation of CFU-macrophage (CFU-M) and proliferation of monocytes in vitro (12). In IL-34–deficient mice, development of Langerhans cells in the skin epidermis and microglia in the CNS is selectively impaired (13). On the basis of the phenotype of mice deficient in M-CSF, GM-CSF or IL-34, each cytokine appears to play a selective role in the development of specific subset of tissue macrophages. However, their role in monocyte development in the BM is still unclear because of considerable overlap in function among the three cytokines.

Study of cytokines in monocyte and macrophage development in human has been largely limited to in vitro assays. Human GM-CSF and IL-3 has been shown to promote formation of CFU-GM when added to the BM cell cultures (14), whereas human M-CSF and

*Interdisciplinary Research Group in Infectious Diseases, Singapore–Massachusetts Institute of Technology Alliance for Research and Technology, Singapore 138602; †Infrastructure, Technology and Translational Division, Institute of Molecular and Cell Biology, Singapore 138673; ‡Department of Microbiology, National University of Singapore, Singapore 119228; §Department of Obstetrics and Gynaecology, KK Women's and Children's Hospital, Singapore 229899; ¶Duke–National University of Singapore Graduate Medical School, Singapore 169857; ‖Experimental Fetal Medicine Group, Department of Obstetrics and Gynaecology, National University of Singapore, Singapore 119228; #Cancer and Stem Cell Biology Program, Duke–National University of Singapore Graduate Medical School, Singapore 169857; **Department of Reproductive Medicine, KK Women's and Children's Hospital, Singapore 229899; ††Department of Biological Engineering, Center for Environmental Health Sciences, Massachusetts Institute of Technology, Cambridge, MA 02139; ‡‡Stem Cell and Developmental Biology, Genome Institute of Singapore, Singapore 138672; and §§Koch Institute for Integrative Cancer Research and Department of Biology, Massachusetts Institute of Technology, Cambridge, MA 02139

[1]Y.L. and Q.C. contributed equally to this work.

Received for publication March 19, 2013. Accepted for publication July 7, 2013.

This work was supported by the National Research Foundation Singapore through the Singapore–Massachusetts Institute of Technology Alliance for Research and Technology's Interdisciplinary Research Group in Infectious Disease research program. J.K.Y.C. received salary support from the National Medical Research Council, Singapore (Grant NMRC/CSA/012/2009).

Y.L., Q.C., and J.C. designed research; Y.L., Q.C., D.Z., L.Y., Y.H.C., and L.H.W. performed research; S.Q.T., T.C.T., J.K.Y.C., S.A., and P.C.D. contributed new reagents/analytic tools; Y.L., Q.C., B.L. and J.C. analyzed data; and Y.L., Q.C., and J.C. wrote the paper.

Address correspondence and reprint requests to Prof. Jianzhu Chen, Koch Institute for Integrative Cancer Research, Massachusetts Institute of Technology, 77 Massachusetts Avenue, Cambridge, MA 02139. E-mail address: jchen@mit.edu

The online version of this article contains supplemental material.

Abbreviations used in this article: BCG, bacillus Calmette–Guérin; BM, bone marrow; CFU-M, CFU-macrophage; DC, dendritic cell; FL, fetal liver; Flt3-L, Flt3 ligand; HSC, hematopoietic stem cell; MPO, myeloperoxidase; NP, nucleocapsid protein; SSC, side scatter.

IL-34 promoted CFU-M formation (13). Recent development of humanized mice has opened up the possibility to study human monocyte and macrophage development in vivo and the role of cytokines in this process. Engraftment of human $CD34^+$ hematopoietic stem/progenitor cells from cord blood or fetal liver (FL) into immunodeficient mice lacking T, B, and NK cells, such as NOD/scid $Il2rg^{-/-}$ (NSG) mice, leads to the generation of various human blood lineage cells in the recipient mice. In these humanized mice, T and B cells are the most robustly reconstituted human cell types, whereas reconstitution of myeloid cells, including monocytes and macrophages, is much less efficient. This is probably because humanized mice are deficient in human M-CSF and GM-CSF, and mouse counterparts do not function on human myeloid precursors (15). Supporting this hypothesis, expression of human M-CSF in humanized mice by hydrodynamic injection of cytokine-encoding plasmid significantly improved the reconstitution of human monocytes in the peripheral blood (16). Similarly, knockin of human M-CSF gene into the corresponding mouse locus in the recipient mice resulted in a significant increase in the circulating human monocytes, although the increase in tissue macrophages was much less (17). In GM-CSF/IL-3 knockin mice, the level of human macrophages in the lungs was selectively increased without apparent increase in human monocytes in the circulation or macrophages in other tissues, consistent with the requirement for GM-CSF and IL-3 for alveolar macrophage development (18). Despite these progresses, it is still unclear at what stage M-CSF and GM-CSF are required for human monocyte development and to what extent the different human cytokines affect tissue macrophage development in vivo.

In this study, we show human monocyte/macrophage development in humanized mice is blocked at the $SSC^{hi}CD14^{lo}CD45^+$ promonocyte stage in the BM. This block can be relieved by either human M-CSF or GM-CSF. However, only M-CSF is capable of stimulating development of phenotypically mature monocytes and tissue macrophages. Furthermore, we show that M-CSF–induced monocytes and macrophages are functional as they responded robustly to challenges by LPS, influenza virus, and *Mycobacterium.* Our study identifies the precise stage at which human monocyte development in humanized mice is blocked and the critical role of M-CSF in the development of circulating monocytes and tissue macrophages. These findings provide definitive evidence to support a critical role of M-CSF and GM-CSF in human monocyte development in the BM and their distinct functions in tissue macrophage development. The enhanced reconstitution and functionality of monocytes/macrophages in the humanized mice following M-CSF expression also provide an in vivo system to investigate the role of macrophages in physiological and pathological processes.

Materials and Methods

Generation of humanized mice and hydrodynamic injection

Human FL samples were obtained from aborted fetuses at 15–23 wk of gestation, in accordance with the institutional ethical guidelines of the National University Hospital of Singapore and KK Women's and Children's Hospital of Singapore. All women gave written informed consent for the donation of their fetal tissue for research. NOD/scid $Il2rg^{-/-}$ (NSG) mice were obtained from The Jackson Laboratory, and maintained under specific pathogen-free conditions in the animal facilities at National University of Singapore. Pups within 48 h of birth were sublethally irradiated (100 cGy) and engrafted with $CD34^+$ FL cells by intracardiac injection (2×10^5 cells/recipient). Human M-CSF (transcript variant 1), GM-CSF, or IL-4 (transcript variant 1) were cloned into pcDNA3.1(+) vector individually. Plasmid DNA was purified by Maxi-prep Kit (Promega) with endotoxin removal. For hydrodynamic injection, 50 μg plasmid in 1.8 ml PBS was injected into 8 wk or older humanized mice within 7 s using a 27-gauge needle. All experiments involving human tissues and mice were approved by the institutional committees at National University of Singapore and Massachusetts Institute of Technology.

Isolation of $CD34^+$ FL cells

To isolate human $CD34^+$ cells, FL tissues were cut into small pieces and digested with collagenase IV (2 mg/ml) at 37°C for 15 min. A single-cell suspension was prepared by passing the digested tissue through a 100-μm cell strainer (BD Biosciences), and $CD34^+$ cells were purified with the RosetteSep system using the CD34-positive selection kit (StemCell Technologies). The purity of $CD34^+$ cells was 90–99%.

Flow cytometry and cell sorting

Single-cell suspensions from the BM, spleen, lungs, and liver were prepared as described previously (16). Cells were stained with the following Abs specific for human CD45 (2D1) and CD34 (581) from BD Biosciences; and CD14 (HCD14), CD16 (3G8), CD33 (WM53), CD117 (104D2), CD11b (ICRF44), CD80 (2D10), CD163 (GHI61), CD68 (Y1-82A), CD66b (G10F5), CD13 (WM15), and mouse CD45.1 (A20) from BioLegend. Stained cells were analyzed by flow cytometry using LSRII, and data were analyzed by FACSDiva (BD Biosciences) or FlowJo (Tree Star). Cell sorting of monocyte/macrophage progenitors from the tibias of the BM was performed using FACSAria cell sorter (BD Biosciences) based on forward scatter (FSC) and side scatter (SSC).

Cell culture and CFU assay

Sorted monocyte/macrophage progenitors from the BM were cultured in RPMI 1640 medium, 10% FCS and supplemented with 50 ng/ml M-CSF for macrophage differentiation or 50 ng/ml GM-CSF and 50 ng/ml IL-4 for DC differentiation. All cytokines were purchased from R&D Systems. For CFU assays, sorted monocyte/macrophage progenitors were plated at 2,000, 5,000, and 10,000 cells/dish in complete MethoCult media (MethoCult H4435 enriched; StemCell Technologies), according to the product manual. Cells were incubated in 35-mm culture dishes at 37°C with 5% CO_2. The numbers of colonies were counted under a stereomicroscope after 14 d in culture.

Histology, cytospin, and Giemsa staining

For histology, mice were intracardiacally perfused with saline buffer for 10 min. Organs were harvested, placed in disposable molds, immersed in OCT, and flash-frozen in liquid nitrogen. The blocks were stored at −80°C until use. Ten-micrometer sections were prepared and stained with anti-human CD68 Ab (KP1) (Abcam) and anti-mouse CD68 Ab (FA-11) (Abcam). Sections were analyzed using the Mirax Midi slider scanner (Zeiss). For H&E stain, livers were embedded in paraffin, and 5-μm-thick sections were prepared. The paraffin sections were stained with H&E and analyzed via a light microscope.

For cytospin, mononuclear cells from blood or organs were isolated by Percoll gradient centrifuge, and 10^5 cells in 100 μl 2% FCS–PBS were added to the cytospin cassette and centrifuged at 1000 rpm for 5 min. The cell smears on polylysine-coated slides were air-dried and fixed with 4% paraformaldehyde. For Ki67 staining, cytospun cells were blocked and stained with rabbit anti-human Ki67 (ab833) (Abcam) and mouse anti-human CD68 (KP1) (Abcam) Abs. Slides were mounted with DAPI and analyzed using the Mirax Midi slider scanner (Zeiss). For Giemsa staining, cells were stained with Giemsa for 5 min and washed with distilled water. The stained slides were examined under a microscope.

RNA extraction and real-time PCR

Total RNA was extracted from lysed tissues or cells with RNeasy Plus Mini kit (Qiagen), according to the manufacturer's instructions. RNA (1 μg) was used for cDNA synthesis with ImProm-II Reverse Transcription System (Promega). Quantitative RT-PCR was performed with the CFX96 Real-Time System (Bio-Rad) using the following gene specific primer pairs: human IL-6 (sense, 5′-AATTCGGTACATCCTCGACGG-3′, and antisense, 5′-TTGGAAGGTTCAGGTTGTTTTCT-3′), human myeloperoxidase (MPO) (sense, 5′-CCAGATCATCACTTACCGGGA-3′, and antisense, 5′-CACTGAGTCATTGTAG-GAACGG-3′), human PU.1 (sense, 5′-ATAGCGACCATTACTGGGACT-3′, and antisense, 5′-GGGTATCGAGGACGTGCAT-3′), human LZM (sense, 5′-ATGGG-AGAGTGGTTACAACACA-3′, and antisense, 5′-CCAGTAGCGGCTATTGATCTGAA-3′), human C/EBPβ (sense, 5′-CTTCAGCCCGTACCTGGAG-3′, and antisense, 5′-GGAGAGGAAGTCGTGGTGC-3′), human c-myb (sense, 5′-CTTCAGCCCGTAC-CTGGAG-3′, and antisense, 5′-AGGCAGTAGCTTTGCGATTTC-3′), and human EGR-1 (sense, 5′-GGTCAGTGGCCTAGTGAGC-3′, and antisense, 5′-GTGCCGCTGAGTAA-ATGGGA-3′). Expression values were calculated by

comparative threshold cycle method and normalized to mouse L32 or human GAPDH.

LPS challenge, influenza virus infection, and bacillus Calmette–Guérin infection

Ten micrograms of LPS (Sigma-Aldrich) in 100 μl PBS was injected i.p. into 10- to 12-wk-old humanized mice. Sera were collected before injection and 2 and 12 h after injection. Concentrations of human inflammatory cytokines in the sera were analyzed by the Cytometric Bead Array System (CBA) (BD Biosciences) on LSRII, according to the manufacturer's instructions, and data were analyzed by FCAP Array software (BD Biosciences).

Influenza A/Puerto Rico/8/34 (H1N1) virus (300 PFU in 75 μl PBS) was administered to anesthetized mice via intratracheal route. Lungs were harvested before infection and 24, 48, and 72 h postinfection. For each mouse, the left lobe was used for single-cell preparation for flow cytometry analysis as described above. The superior lobe of right lung was cut to extract RNA for quantitative RT-PCR analysis. The remaining of the three right lobes were weighed and homogenized in ice-cold HBSS with 0.1% BSA (100 mg tissue/ml). The lung homogenates were centrifuged at 10,000 × *g* for 10 min at 4°C to collect the supernatants for CBA assay to measure the cytokine levels as above.

Mycobacterium bovis bacillus Calmette–Guérin (BCG) strain Pasteur 1173P2 (American Type Culture Collection, Manassas, VA) was grown in 7H9 culture medium at 37°C in an 850-cm^2 polystyrene roller bottle (Corning) at 10 rpm. When the culture reached an OD (OD_{600}) of 0.6, bacilli were harvested. Each mouse was injected i.p. with 5×10^6 CFU BCG in 0.5 ml. Before infection and at 24 and 72 h postinfection, the peritoneum was flushed with 5 ml PBS, and the spleen was homogenized in 10 ml PBS. The lavage and tissue homogenate were serially diluted in triplicates in 7H9 medium and plated on 7H11 agar. The plates were kept in incubator, and the numbers of colonies were counted after 4 wk. The rest of the peritoneal lavage was centrifuged to obtain cells for flow cytometry analysis and to extract RNA for quantitative RT-PCR analysis as described above.

Statistical analysis

Data are presented as mean and SEM. The nonparametric Mann–Whitney *U* test was used to analyze the differences between two groups. A p value < 0.05 was considered as statistically significant.

Results

Human monocyte development is blocked at the promonocyte stage in the BM of humanized mice

Humanized mice were constructed by intracardiac injection of sublethally irradiated newborn NSG pups with CD34$^+$ human FL cells. Twelve weeks later, the peripheral blood, spleen, BM, lungs, and liver were analyzed for the presence of human CD14$^+$CD11b$^+$ monocytes/macrophages. The average percentages of CD14$^+$ CD11b$^+$ cells among the human CD45$^+$ leukocyte population were 5.0 ± 0.5% in the blood, 0.7 ± 0.06% in the spleen, 20.2 ± 1.7% in the lung, 5.7 ± 1.3% in the liver, and 19.0 ± 5.2 in the BM (Fig. 1A, Table I). To determine whether mature tissue-resident macrophages were generated in humanized mice, we analyzed the expression of macrophage marker CD68 by human CD14$^+$ cells in the spleen, BM, lungs, and liver. Most CD14$^+$ cells were negative for CD68 (Fig. 1B). These data suggest that reconstitution of human monocytes/macrophages in humanized mice is poor, consistent with previous reports (15, 19).

We noticed in the BM a unique cell population with high SSC (Fig. 1C) and a significant human cell population with a low level of CD14, a high level of CD11b but negative for CD68 (CD14^{lo} CD11b^{hi}CD68$^-$) (Fig. 1A, 1B). To determine the relationship between these two populations, the CD14^{lo} cells were gated and analyzed for FSC and SSC. More than 80% of CD14^{lo} cells were

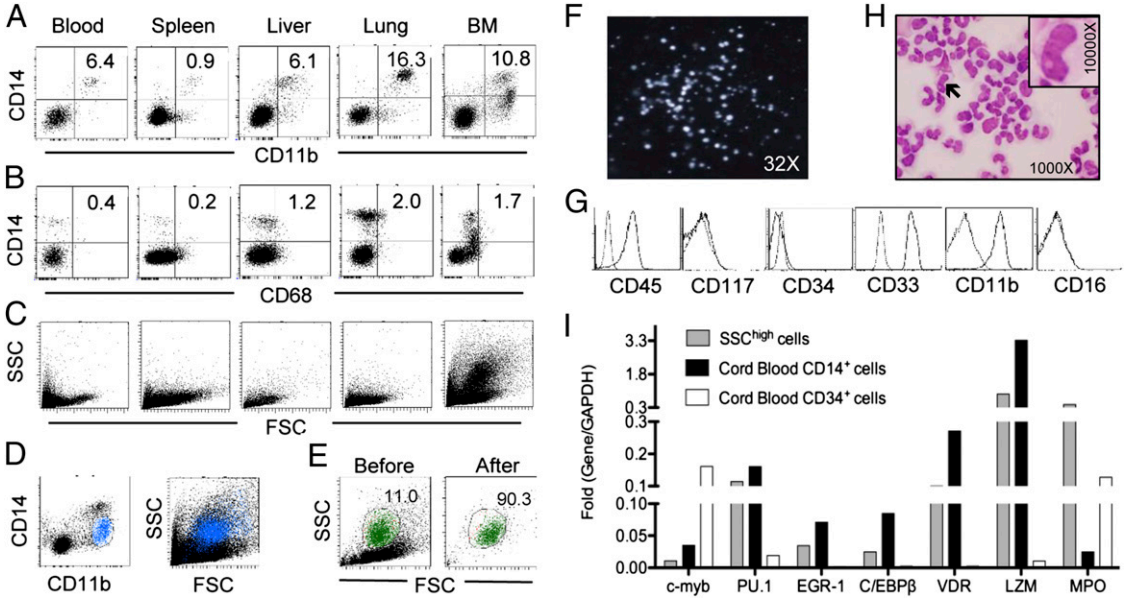

FIGURE 1. Characterization of the SSC^{hi} human cells in the BM of humanized mice. Cells from PBMC, spleen, lungs, liver, and BM of 12-wk-old humanized mice were analyzed. Cells were stained for human CD45, CD14, plus CD11b or CD68 and analyzed by flow cytometry. (**A**) Shown are CD14 versus CD11b staining profiles. (**B**) CD14 versus CD68 staining profile gated on human CD45$^+$ cells. (**C**) SSC versus FSC profiles of total live cells in the various tissues. (**D**) CD14 versus CD11b (*left panel*) and SSC versus FSC (*right panel*) profiles of human CD45$^+$ cells from the BM. The CD14^{lo}CD11b$^+$ population was shown as blue. (**E**) Comparison of SSC versus FSC profiles of BM cells before (*left panel*) and after purification by cell sorting (*right panel*). Data are representative of five independent experiments. (**F**) Sorted SSC^{hi} cells were cultured in triplicate in complete MethoCult for 14 d. Colonies were examined and enumerated under a steromicroscope. A representative large CFU-M colony is shown from three independent experiments. (**G**) Sorted SSC^{hi} cells were stained for human CD45, CD117, CD34, CD33, CD11b, and CD16 (black lines) and analyzed by flow cytometry and compared with unstained controls (dash lines). Data are representative of three independent experiments. (**H**) Giemsa stain of sorted SSC^{hi} cells. Representative image is shown from one of three samples. *Inset*, A higher magnification of the arrow-pointed cell. The numbers indicate magnifications. (**I**) RNA isolated from purified SSC^{hi} cells, cord blood CD45$^+$CD14$^+$ cells, and cord blood CD45$^+$CD34$^+$ cells were analyzed by quantitative RT-PCR to measure the levels of human c-myb, PU.1, EGR1, C-EBPβ, VDR, LZM, and MPO transcripts. Shown are the mean values of duplicate samples. Input cDNA was normalized according to GAPDH expression levels. Data are representative of two independent experiments.

Table I. Quantification of human monocytes and macrophages in different organs of humanized mice with or without cytokine treatment

	Control Mice		M-CSF–Treated Mice		GM-CSF–Treated Mice		IL-4–Treated Mice	
Tissue	$CD14^+$ $CD11b^+$	$CD14^+$ $CD68^+$	$CD14^+$ $CD11b^+$	$CD14^+$ $CD68^+$	$CD14^+$ $CD11b^+$	$CD14^+$ $CD68^+$	$CD14^+$ $CD11b^+$	$CD14^+$ $CD68^+$
Blood	4.9 ± 0.5	0.6 ± 0.2	31.6 ± 5.2	3.7 ± 0.7	12.5 ± 3.1	1.6 ± 0.2	4.0 ± 1.4	1.7 ± 0.6
Spleen	0.7 ± 0.1	0.3 ± 0.1	19.7 ± 7.3	11.7 ± 5.9	2.9 ± 0.6	0.7 ± 0.2	0.5 ± 0.0	0.3 ± 0.0
Liver	5.7 ± 1.3	1.0 ± 0.0	56.8 ± 5.9	30.9 ± 10.2	24.2 ± 5.5	10.2 ± 2.4	3.2 ± 0.7	1.8 ± 0.9
Lung	20.2 ± 1.7	2.9 ± 0.8	62.2 ± 9.4	28.4 ± 6.4	36.5 ± 0.1	17.1 ± 0.8	11.2 ± 2.1	4.7 ± 0.5
BM	16.4 ± 4.0	3.3 ± 0.7	19.0 ± 5.2	8.4 ± 5.2	17.2 ± 3.5	3.6 ± 1.1	5.3 ± 1.0	2.0 ± 0.4

Humanized mice engrafted with $CD34^+$ FL cells from the same donors were either untreated (control) or treated with M-CSF, GM-CSF, or IL-4. Cells from the indicated tissues were stained for human CD45, CD14, plus CD11b or CD68, followed by flow cytometry analysis. Shown are the mean percentages and SEMs of human $CD14^+CD11b^+$ and $CD14^+CD68^+$ cells among $CD45^+$ human cells in the blood, spleen, liver, lung, and BM. Data shown are from eight mice per group.

high for SSC (Fig. 1D), indicating that the cells in these two populations are mostly the same. On average, $\sim 3 \times 10^6$ $CD14^{lo}$ SSC^{hi} cells were recovered from one femur, representing ~10% of human cells in the BM. Thus, although the frequency of $CD14^+$ human monocytes/macrophages is low in the blood and tissues, there is a significant accumulation of $CD14^{lo}SSC^{hi}$ monocytic cells in the BM, suggesting a possible block of human monocyte development in the BM.

To define the developmental stage of $CD14^{lo}SSC^{hi}$ cells in the BM of humanized mice, SSC^{hi} cells were purified (>90%) (Fig. 1E) and used in a series of analysis. We performed the colony-forming cell assay to determine the frequency and types of progenitors present in the population. Cells were plated in enriched MethoCult, which supports the optimal growth of erythroid progenitors and granulocyte/macrophage progenitors. After 2 wk of culture, only CFU-M was detected, and the frequency was low (1/220) (Fig. 1F), suggesting that SSC^{hi} cells in the BM are primarily late-stage myeloid progenitors.

The purified SSC^{hi} cells exhibited a phenotype of $CD45^+CD34^-CD117^-CD33^+CD11b^+CD14^{lo}CD16^-$ (Fig. 1D, 1G), resembling the surface phenotype of promonocytes (Supplemental Fig. 1) (20). Giemsa staining of the purified SSC^{hi} cells showed that majority of these cells had an indented nucleus with clearly visible nucleolus (Fig. 1H), which is also a characteristic of promonocyte. Quantitative RT-PCR analysis revealed that the SSC^{hi} cells expressed human myeloid–specific genes, including PU.1, EGR-1, VDR, and LZM (Fig. 1I), although the levels were lower than those in cord blood $CD14^+$ monocytes but much higher than the levels in cord blood $CD34^+$ progenitor cells. Compared with the cord blood $CD34^+$ progenitor cells, the SSC^{hi} cells had a lower level of expression of early myeloid commitment gene c-myb and a higher level of expression of myeloid differentiation gene C-EBPβ, suggesting that the SSC^{hi} cells are at the postmonoblast stage (Supplemental Fig. 1) (21). In addition, the level of MPO was much higher in SSC^{hi} cells than in cord blood $CD14^+$ monocytes. Because the expression of MPO is downregulated after monocyte maturation, the relatively high level of MPO expression by the SSC^{hi} cells suggests that they are still at the immature stage (Supplemental Fig. 1) (22). Taken together, these data suggest that the $CD14^{lo}SSC^{hi}$ human cells in the BM are promonocytes. Hence, human monocyte/macrophage development is blocked at the promonocyte stage in the BM of humanized mice.

GM-CSF and M-CSF treatment promotes the release of promonocytes from the BM of humanized mice

To stimulate further development of human promonocytes in the BM of humanized mice, we expressed human M-CSF or GM-CSF in mice by hydrodynamic delivery of cytokine-encoding plasmids through tail vein injection. Seven days after M-CSF or GM-CSF plasmid injection, the SSC^{hi} population disappeared from the BM (Fig. 2A). As a control, expression of human IL-4 did not affect the level of the SSC^{hi} population in the BM of humanized mice. Notably, the frequencies of $CD14^+$ monocytes were significantly increased in the blood, spleen, liver, and lungs of M-CSF– or GM-CSF–treated mice as compared with untreated or IL-4–treated mice (Fig. 2B, Table I). Compared with those in M-CSF–treated mice, a significant fraction of monocytes/macrophages in GM-CSF–treated mice remained $CD14^{lo}$. These results suggest that although both M-CSF and GM-CSF can promote the release of promonocytes from the BM, M-CSF is required for the terminal differentiation of human promonocytes.

On the basis of the lack of CD16 expression (Fig. 1G), the SSC^{hi} population is unlikely to include granulocytic precursors. To further exclude this possibility, we assayed for induction of granulocytes following hydrodynamic expression of G-CSF, Flt3 ligand (Flt3-L), GM-CSF, and M-CSF. No significant increase in the frequency of $CD13^+CD66b^+$ granulocytes was detected in the blood of humanized mice 7 d postcytokine expression (Supplemental Fig. 2C).

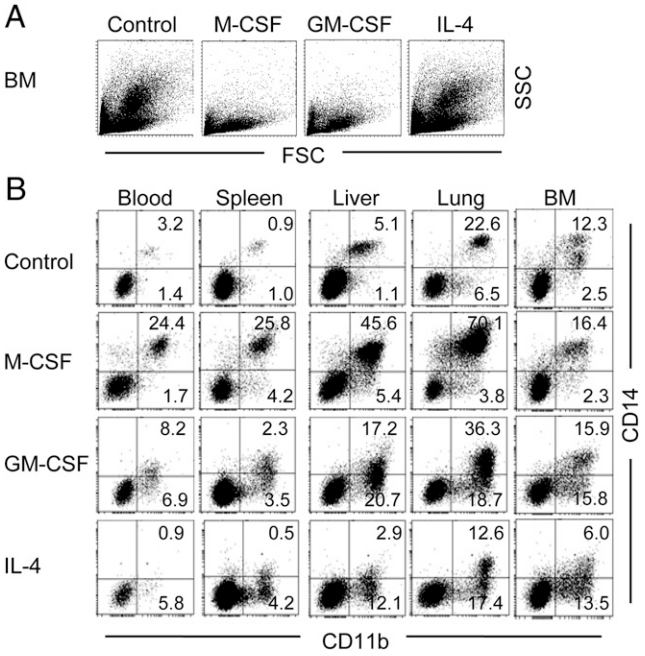

FIGURE 2. Differentiation of promonocytes in response to human M-CSF and GM-CSF in humanized mice. pcDNA plasmids encoding M-CSF, GM-CSF, or IL-4 were hydrodynamically injected into humanized mice. Seven days after injection, single-cell suspensions were prepared from the indicated tissues and stained for human CD45, CD14, and CD11b and analyzed by flow cytometry. (**A**) SSC versus FSC profiles of total BM cells. (**B**) CD14 versus CD11b staining profiles gating on human $CD45^+$ cells from blood, the spleen, liver, lungs, and BM. The numbers indicate the percentages of cells in the gated regions. Data are representative of three independent experiments with a total of nine mice per group.

Unlike GM-CSF– or M-CSF–treated mice, expression of G-CSF or Flt3-L neither abolished the accumulation of SSC^{hi} population in the BM nor improved the monocyte reconstitution in the blood (Supplemental Fig. 2A, 2B). These data further support the designation of the $SSC^{hi}CD14^{lo}$ cells as promonocytes.

M-CSF treatment induces development of tissue resident macrophages in humanized mice

We further analyzed the development of tissue resident human macrophages in M-CSF–treated mice. Following perfusion, the spleen, liver, and lungs were harvested, and cells were analyzed by flow cytometry. The majority of $CD14^+$ cells in the spleen, liver, and lungs of M-CSF–treated mice were positive for macrophage markers CD68 and CD163 (Fig. 3A). Interestingly, although the frequency of blood $CD14^+$ cells was increased in M-CSF–treated mice (Table I), they remained CD68 negative, consistent with the notion that monocytes acquire macrophage phenotype as they enter tissues (23). Considerable numbers of mouse, but not human, $CD68^+$ macrophages were detected in the lung and liver sections of untreated humanized mice (Fig. 3B), whereas in M-CSF–treated mice both mouse and human $CD68^+$ macrophages were detected, and they had similar numbers and distributions in the same tissue (Fig. 3C). To further determine the localization of human macrophages in the liver, we stained paraffin-fixed liver sections from M-CSF–treated mice with H&E and frozen liver sections with anti-human CD68. High-resolution image analysis revealed that human macrophages primarily occupied sinusoidal spaces, the same as mouse Kupffer cells (Supplemental Fig. 3A). These results show that M-CSF stimulates development of human promonocytes in the BM into fully matured tissue-resident macrophages in humanized mice.

In a recent study, IL-4 was shown to induce alternatively activated macrophages, which are generated by local macrophage proliferation rather than maturation from circulating monocytes (24). However, expression of IL-4 in humanized mice neither reduced the accumulation of promonocytes in the BM nor promoted the generation of human $CD68^+$ macrophages in the tissues (Fig. 2A, Supplemental Fig. 3B). To test whether local proliferation of macrophages in the presence of M-CSF may contribute to the generation of tissue macrophages in the cytokine-treated mice, mononuclear cells from the blood, spleen, liver, and lungs of M-CSF–treated mice were cytospun and stained for the proliferation marker Ki67 and human CD68. Consistent with results from Fig. 3A, very few $CD68^+$ cells were detected in the blood but a significant fraction stained positive from the spleen, liver, and lungs (Fig. 3D). However, none of the 1000 $CD68^+$ cells counted was stained positive for Ki67. Thus, neither IL-4 nor local proliferation contribute significantly to the reconstitution of human $CD68^+$ macrophages in the tissues.

M-CSF–treated mice mount stronger responses to LPS, influenza virus, and BCG

To determine whether the M-CSF-induced human monocytes/macrophages are functional, we tested their ability to produce proinflammatory cytokines in response to LPS. Humanized mice with or without M-CSF treatment were bled before and 2 and 12 h after LPS challenge, and the serum levels of human cytokines were measured. Significantly elevated levels of human IL-6, TNF-α, IL-1β, IL-8, and IL-10 were detected in the M-CSF–treated mice but not in untreated mice (Supplemental Fig. 4A). Of note, the basal levels of these cytokines were the same between M-CSF–treated mice and untreated mice (before LPS challenge), indicating that the induction of cytokines is not due to M-CSF expression. Thus, the M-CSF–induced human monocytes and macrophages are quiescent and can be activated to produce inflammatory cytokines following LPS stimulation.

To test whether human macrophages in M-CSF–treated mice can respond to influenza A virus infection, untreated and M-CSF–treated humanized mice were infected intratracheally with influenza A/Puerto Rico/8/34 (PR8) virus, and sacrificed at 24, 48, and

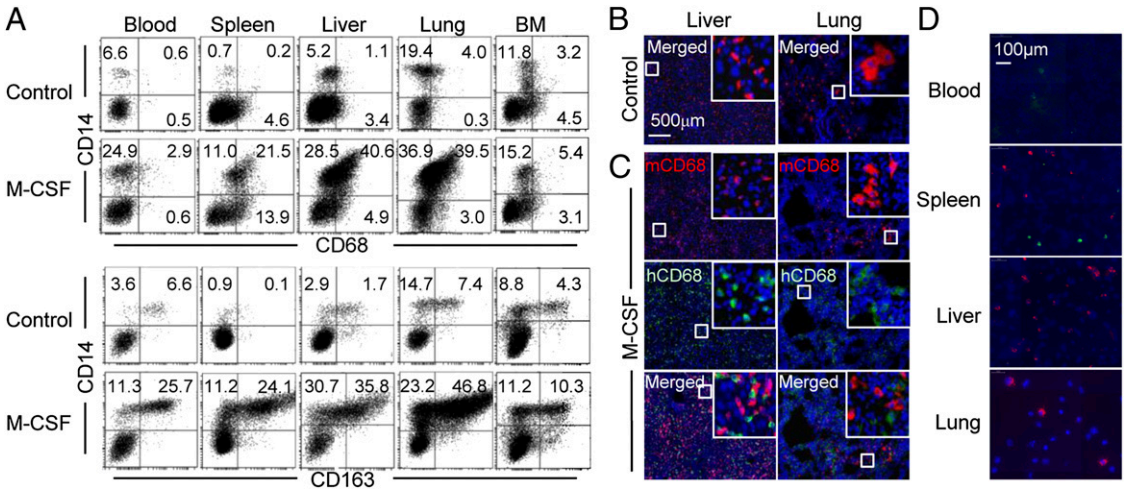

FIGURE 3. Development of tissue-resident human macrophages in M-CSF–treated mice. (**A**) Improved reconstitution of tissue-resident human macrophages. Humanized mice were hydrodynamically injected with M-CSF encoding plasmid. Seven days after injection, single-cell suspension was prepared from indicated tissues and stained for human CD45, CD14, CD68, and CD163. Shown are CD14 versus CD68 (*upper panel*) and CD14 versus CD163 (*lower panel*) staining profiles gating on $CD45^+$ human cells. The numbers indicate the percentages of cells in the gated regions. Data are representative of three independent experiments with a total of nine mice per group. (**B** and **C**) Comparison of immunofluorescence staining of mouse and human macrophages in the lung and liver of untreated humanized mice (B) and M-CSF–treated mice (C). Lungs and liver were snap-frozen, cryosectioned, stained for human CD68 (green) and mouse CD68 (red), and scanned by microscopy. Merged images are shown for sections from untreated humanized mice (B). Single-color and merged images are shown for sections from M-CSF–treated mice. *Insets*, Higher magnification of the boxed areas. Representative images are shown from one of five mice per group. Scale is indicated. (**D**) Seven days after injection of M-CSF plasmid, mononuclear cells from the blood, spleen, liver, and lungs were cytospun onto glass slides and stained for Ki67 (green), human CD68 (red), and DAPI (blue). Representative images are shown from one of five mice in two independent experiments.

72 h postinfection. The level of viral replication in the lungs was measured by quantitative PCR of viral nucleocapsid protein (NP) transcript and normalized to the mouse ribosomal L32 transcript. The level of viral NP transcript was significantly lower in the M-CSF–treated mice than in untreated mice at 24 and 48 h postinfection (Fig. 4A). Significantly more human macrophages and other human leukocytes were recovered from the lungs of M-CSF–treated mice than untreated mice at all three time points postinfection (Supplemental Fig. 4B). The percentages of human macrophages that upregulated costimulatory molecule CD80 was also significantly higher in M-CSF–treated mice than untreated mice at 24 h postinfection (Supplemental Fig. 4C). Furthermore, significantly higher levels of human IL-6, TNF-α, and IL-1β were detected in the lung homogenates of M-CSF–treated mice than untreated mice at 48 h postinfection (Fig. 4B). Thus, better human macrophage reconstitution in the lungs of M-CSF–treated mice is associated with an enhanced human immune response to influenza virus infection.

We further evaluated human macrophage response to *Mycobacterium* BCG, which has served as a classic model for studying macrophage activation and migration (25). Both untreated and M-CSF–treated mice were injected i.p. with 5×10^6 CFU BCG and peritoneal lavage, and spleen homogenates were prepared 24 and 72 h later for BCG colony–forming assay. Significantly lower numbers of BCG colony counts were observed in the spleen and peritoneal lavage of M-CSF–treated mice than untreated mice (Fig. 4C). Human $CD14^+CD11b^+$ macrophages were detected in the peritoneal lavage of M-CSF–treated mice 24 h postinfection but not in untreated mice or M-CSF–treated mice before BCG infection (Fig. 4D). These data suggest that human monocytes/macrophages can be recruited to the site of BCG infection in M-CSF–treated mice.

Discussion

The ability to study human monocyte and macrophage development in an in vivo setting is a unique advantage of humanized mice. In this study, we report that human monocyte/macrophage development is blocked at the promonocyte stage in the BM of humanized mice. Expression of either human M-CSF or GM-CSF releases the block and M-CSF further promotes development of promonocytes into mature monocytes in the circulation and tissue-resident macrophages. The M-CSF–induced monocytes/macrophages are functional as they readily respond to LPS stimulation and influenza virus and BCG infection. These findings reveal the stage at which M-CSF or GM-CSF is required for human monocyte/macrophage development and provide an in vivo system for studying the role of human monocytes/macrophages in immunity and pathogenesis.

The role of cytokines in monocyte development in the BM, especially in human, is still unclear. On the basis of the relatively normal numbers of monocytes in the peripheral blood of GM-CSF– or IL-34–deficient mice, both GM-CSF and IL-34 do not appear to be required for monocyte development in the mouse. The role of M-CSF in monocyte development, however, is more controversial. Early studies reported that the number of monocytes was reduced in the blood of M-CSF–deficient mice probably because of a deficiency of osteoclasts that are required to maintain a functional BM microenvironment (2, 4, 10, 26–28). A later study showed that M-CSF was critical for the survival of circulating monocytes in the periphery (29). A recent study, however, reported that the number of circulating monocytes was not reduced in M-CSF–deficient mice (6). Consistently, Ab blocking of CSF1R in mice selectively inhibited monocyte maturation in the periphery without affecting their numbers (30). Despite these discrepancies, current evidence suggests that M-CSF is likely involved in the maturation and survival rather than the production of monocytes in mice.

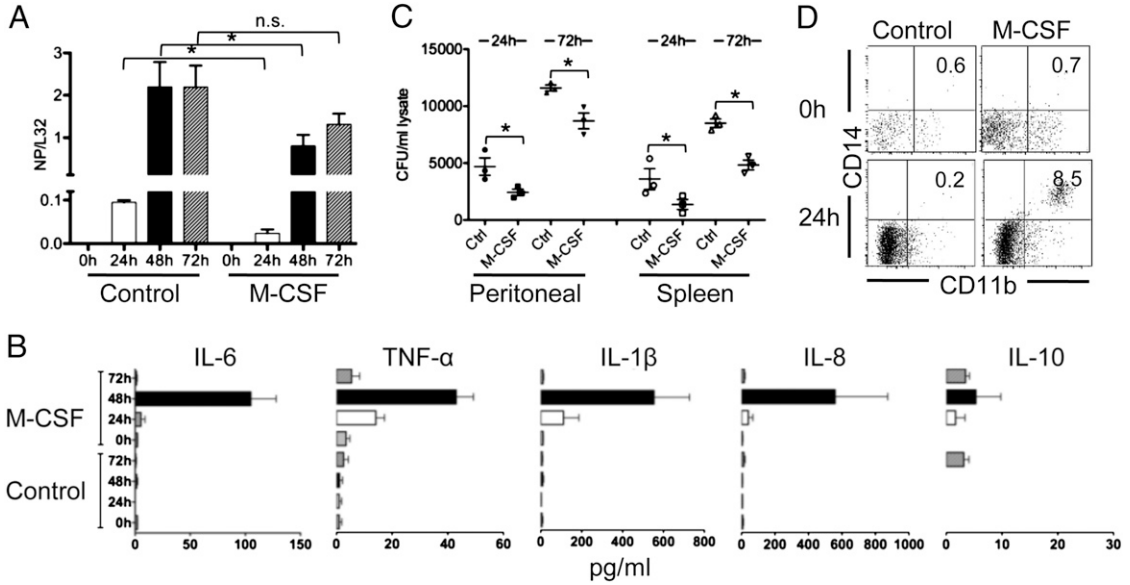

FIGURE 4. Influenza virus and BCG infection in M-CSF–treated mice. (**A** and **B**) M-CSF–treated and untreated mice were infected intratracheally with 300 PFU PR8 virus. Lungs were harvested before infection (0 h) and 24, 48, and 72 h postinfection. The levels of viral NP transcript was measured by quantitative RT-PCR and normalized to the level of mouse L32 transcript (A). CBA assay of human IL-6, TNF-α, IL-1β, IL-8, and IL-10 in lung homogenates from untreated and M-CSF–treated humanized mice (B). Shown are the mean values and SEM of three mice per group. Data are representative of two independent experiments. $*p < 0.05$. (**C** and **D**) M-CSF–treated mice and untreated mice were infected i.p. with BCG. Peritoneal lavage and spleen were collected 24 and 72 h postinfection. Comparison of BCG colony counts from peritoneal lavage and the spleen of untreated and M-CSF–treated humanized mice at 24 and 72 h postinfection (C). Each symbol represents colony counts from an individual mouse; horizontal bars indicate the mean values. Error bars indicate SEM. $*p < 0.05$. Peritoneal cells from untreated and M-CSF–treated humanized mice before and 24 h postinfection were stained for human CD45, CD14, and CD11b. CD14 versus CD11b staining profiles are shown for $CD45^+$ human cells (D). The numbers indicate percentages of cells in the gated areas.

Our studies in humanized mice show that human monocyte/macrophage development is blocked at the $CD14^{lo}SSC^{hi}$ promonocyte stage in the BM because of the lack of human M-CSF and GM-CSF. Expression of either M-CSF or GM-CSF leads to the release of promonocytes from the BM, suggesting that M-CSF and GM-CSF have overlapping function in the generation of monocytes. M-CSF and GM-CSF could directly drive the differentiation of promonocytes or provide survival signals to promonocytes to respond to other internal and external cues for further differentiation into circulating monocytes (29). Because provision of Flt3-L did not stimulate promonocyte differentiation, Flt3-L is unlikely involved in this process. In our study, we did not test the effect of IL-34. It is possible that IL-34 may have the similar function as M-CSF and GM-CSF considering they all promote monocyte proliferation in vitro. The fact that human promonocytes accumulated in the mouse BM suggests that mouse cytokines do not replace human cytokines in this process, consistent with the observations that mouse M-CSF and GM-CSF do not react with human cells (15). Because the BM microenvironment is unlikely impaired in humanized mice, our findings reveal a direct role of M-CSF and GM-CSF in human monocyte development in the BM and suggest that M-CSF and GM-CSF may function differently between mouse and human.

For a long time, tissue macrophages are thought to be derived from circulating monocytes as donor-derived monocytes contribute to tissue macrophages following BM transplantation (31). Recently, however, accumulating evidence suggests that macrophages in many tissues, such as the brain and liver, are maintained by self-renewal, independent of circulating monocytes (24, 31–33). Following expression of human M-CSF in humanized mice, human macrophages are induced and take up residence at the same location in the liver and the lungs as the mouse macrophages. We further show that M-CSF–induced $CD68^+$ macrophages did not proliferate in the tissues. In addition, IL-4, which is known to induce alternatively activated macrophages (24), did not reduce the accumulation of promonocytes in the BM or promote the generation of human $CD68^+$ macrophages in the tissues (Figs. 1A, 1B, 3). Thus, the mature tissue macrophages in M-CSF–treated humanized mice are likely generated from further differentiation of circulating monocytes rather than from proliferation of newly generated macrophages in the tissues. Compared with M-CSF–treated mice, where tissue macrophages were mature ($CD14^{hi}CD68^+$), in GM-CSF– and IL-4–treated mice, although human $CD11b^+$ cells were found in the tissues, they remained $CD14^{lo}$ and $CD68^-$ (Fig. 3; Supplemental Fig. 3B). Taken together, these findings show that M-CSF, but not GM-CSF and IL-4, promotes further differentiation of circulating human monocytes into mature tissue macrophages.

There have been significant efforts to improve human monocyte/macrophage reconstitution in humanized mice. The reconstitution level and function of monocytes/macrophages in the M-CSF–treated humanized mice compare favorably to those reported recently using different approaches. Human GM-CSF, IL-3, and M-CSF genes have been used to replace the corresponding mouse genes in BALB/c $Rag2^{-/-}\gamma c^{-/-}$ mice. In M-CSF knockin mice, the level of human $CD14^+$ monocytes in the circulation was increased ~6-fold, reaching 30% of human $CD45^+$ cells, whereas the highest level of tissue macrophage reconstitution was still under 5% of human $CD45^+$ cells (17). In GM-CSF/IL-3 knockin mice, the level of human macrophages in the lungs was increased without apparent increase in human monocytes in the circulation or macrophages in other tissues (17, 18). In comparison, following expression of M-CSF, circulating monocytes were increased ~10-fold in humanized mice, and the significant levels of human macrophages were also detected in the spleen, liver, and lungs, reaching 20–70% of human leukocytes in these tissues. We further show that M-CSF–induced macrophages are mature as they express CD68 and have similar distribution pattern as endogenous mouse macrophages in the liver and lungs, whereas monocytes in the blood did not express CD68 in M-CSF–treated mice, as expected. Compared with the cytokine gene knockin mice where human cytokines were ~50 pg/ml in the mouse serum (17), the more efficient induction of human monocytes and macrophages following hydrodynamic expression of M-CSF is probably due to the high level of human cytokine that was produced (2.5 ng/ml in serum at 24 h postinjection).

We carried out a series of analyses to show that M-CSF–induced human macrophages are functional. Following LPS stimulation, low levels (~300 pg/ml) of human IL-6 and TNF-α were induced in the sera of humanized M-CSF knockin mice (17). In humanized GM-CSF/IL-3 knockin mice, the level of human IL-6 reached ~6000 pg/ml (18). In comparison, we detected much higher levels of IL-6 and TNF-α (~70,000 pg/ml) following LPS challenge in M-CSF–treated humanized mice. We also detected high levels of IL-8 (35,000 pg/ml) and IL-1β (2,000 pg/ml). When GM-CSF/IL-3 knockin mice were challenged with influenza virus, induction of human IL-6 was detected by ELISA and TNF-α and IFN transcripts by RT-PCR. However, no difference in virus replication in the lungs was observed in the presence of human macrophages. In our M-CSF–treated humanized mice, besides induction of significant levels of IL-6, TNF-α, and IL-1β, the virus replication was significantly lower in M-CSF–treated than in nontreated humanized mice. Furthermore, BCG counts were also significantly lower in the spleen and peritoneum in M-CSF–treated than in nontreated humanized mice. The decrease in bacterial counts in the peritoneum was associated with migration of human macrophages to the site of infection. Taken together, our results show that expression of M-CSF in humanized mice promote development of functional monocytes and tissue macrophages.

Acknowledgments

We thank Hooi Linn Loo and Siew Chin Loh for technical support, Drs. Roderick Bronson and Mandeep Kaur for helping with analysis of macrophage localization in the liver, Dr. Farzad Olfat for general program support, and members of Chen Lab for discussion.

Disclosures

The authors have no financial conflicts of interest.

References

1. Stanley, E. R., G. Hansen, J. Woodcock, and D. Metcalf. 1975. Colony stimulating factor and the regulation of granulopoiesis and macrophage production. *Fed. Proc.* 34: 2272–2278.
2. Yoshida, H., S. Hayashi, T. Kunisada, M. Ogawa, S. Nishikawa, H. Okamura, T. Sudo, L. D. Shultz, and S. Nishikawa. 1990. The murine mutation osteopetrosis is in the coding region of the macrophage colony stimulating factor gene. *Nature* 345: 442–444.
3. Cecchini, M. G., M. G. Dominguez, S. Mocci, A. Wetterwald, R. Felix, H. Fleisch, O. Chisholm, W. Hofstetter, J. W. Pollard, and E. R. Stanley. 1994. Role of colony stimulating factor-1 in the establishment and regulation of tissue macrophages during postnatal development of the mouse. *Development* 120: 1357–1372.
4. Wiktor-Jedrzejczak, W., M. Z. Ratajczak, A. Ptasznik, K. W. Sell, A. Ahmed-Ansari, and W. Ostertag. 1992. CSF-1 deficiency in the op/op mouse has differential effects on macrophage populations and differentiation stages. *Exp. Hematol.* 20: 1004–1010.
5. Naito, M., S. Hayashi, H. Yoshida, S. Nishikawa, L. D. Shultz, and K. Takahashi. 1991. Abnormal differentiation of tissue macrophage populations in 'osteopetrosis' (op) mice defective in the production of macrophage colony-stimulating factor. *Am. J. Pathol.* 139: 657–667.
6. Dai, X. M., X. H. Zong, V. Sylvestre, and E. R. Stanley. 2004. Incomplete restoration of colony-stimulating factor 1 (CSF-1) function in CSF-1-deficient Csf1op/Csf1op mice by transgenic expression of cell surface CSF-1. *Blood* 103: 1114–1123.

7. Shibata, Y., Z. Zsengeller, K. Otake, N. Palaniyar, and B. C. Trapnell. 2001. Alveolar macrophage deficiency in osteopetrotic mice deficient in macrophage colony-stimulating factor is spontaneously corrected with age and associated with matrix metalloproteinase expression and emphysema. *Blood* 98: 2845–2852.
8. Nilsson, S. K., G. J. Lieschke, C. C. Garcia-Wijnen, B. Williams, D. Tzelepis, G. Hodgson, D. Grail, A. R. Dunn, and I. Bertoncello. 1995. Granulocyte-macrophage colony-stimulating factor is not responsible for the correction of hematopoietic deficiencies in the maturing op/op mouse. *Blood* 86: 66–72.
9. Ryan, G. R., X. M. Dai, M. G. Dominguez, W. Tong, F. Chuan, O. Chisholm, R. G. Russell, J. W. Pollard, and E. R. Stanley. 2001. Rescue of the colony-stimulating factor 1 (CSF-1)-nullizygous mouse (Csf1(op)/Csf1(op)) phenotype with a CSF-1 transgene and identification of sites of local CSF-1 synthesis. *Blood* 98: 74–84.
10. Wiktor-Jedrzejczak, W. W., A. Ahmed, C. Szczylik, and R. R. Skelly. 1982. Hematological characterization of congenital osteopetrosis in op/op mouse: possible mechanism for abnormal macrophage differentiation. *J. Exp. Med.* 156: 1516–1527.
11. Stanley, E., G. J. Lieschke, D. Grail, D. Metcalf, G. Hodgson, J. A. Gall, D. W. Maher, J. Cebon, V. Sinickas, and A. R. Dunn. 1994. Granulocyte/macrophage colony-stimulating factor-deficient mice show no major perturbation of hematopoiesis but develop a characteristic pulmonary pathology. *Proc. Natl. Acad. Sci. USA* 91: 5592–5596.
12. Lin, H., E. Lee, K. Hestir, C. Leo, M. Huang, E. Bosch, R. Halenbeck, G. Wu, A. Zhou, D. Behrens, et al. 2008. Discovery of a cytokine and its receptor by functional screening of the extracellular proteome. *Science* 320: 807–811.
13. Wang, Y., K. J. Szretter, W. Vermi, S. Gilfillan, C. Rossini, M. Cella, A. D. Barrow, M. S. Diamond, and M. Colonna. 2012. IL-34 is a tissue-restricted ligand of CSF1R required for the development of Langerhans cells and microglia. *Nat. Immunol.* 13: 753–760.
14. Emerson, S. G., Y. C. Yang, S. C. Clark, and M. W. Long. 1988. Human recombinant granulocyte-macrophage colony stimulating factor and interleukin 3 have overlapping but distinct hematopoietic activities. *J. Clin. Invest.* 82: 1282–1287.
15. Manz, M. G. 2007. Human-hemato-lymphoid-system mice: opportunities and challenges. *Immunity* 26: 537–541.
16. Chen, Q., M. Khoury, and J. Chen. 2009. Expression of human cytokines dramatically improves reconstitution of specific human-blood lineage cells in humanized mice. *Proc. Natl. Acad. Sci. USA* 106: 21783–21788.
17. Rathinam, C., W. T. Poueymirou, J. Rojas, A. J. Murphy, D. M. Valenzuela, G. D. Yancopoulos, A. Rongvaux, E. E. Eynon, M. G. Manz, and R. A. Flavell. 2011. Efficient differentiation and function of human macrophages in humanized CSF-1 mice. *Blood* 118: 3119–3128.
18. Willinger, T., A. Rongvaux, H. Takizawa, G. D. Yancopoulos, D. M. Valenzuela, A. J. Murphy, W. Auerbach, E. E. Eynon, S. Stevens, M. G. Manz, and R. A. Flavell. 2011. Human IL-3/GM-CSF knock-in mice support human alveolar macrophage development and human immune responses in the lung. *Proc. Natl. Acad. Sci. USA* 108: 2390–2395.
19. Tanaka, S., Y. Saito, J. Kunisawa, Y. Kurashima, T. Wake, N. Suzuki, L. D. Shultz, H. Kiyono, and F. Ishikawa. 2012. Development of mature and functional human myeloid subsets in hematopoietic stem cell-engrafted NOD/SCID/IL2rγKO mice. *J. Immunol.* 188: 6145–6155.
20. van Lochem, E. G., V. H. van der Velden, H. K. Wind, J. G. te Marvelde, N. A. Westerdaal, and J. J. van Dongen. 2004. Immunophenotypic differentiation patterns of normal hematopoiesis in human bone marrow: reference patterns for age-related changes and disease-induced shifts. *Cytometry B Clin. Cytom.* 60: 1–13.
21. Valledor, A. F., F. E. Borràs, M. Cullell-Young, and A. Celada. 1998. Transcription factors that regulate monocyte/macrophage differentiation. *J. Leukoc. Biol.* 63: 405–417.
22. Lübbert, M., W. Brugger, R. Mertelsmann, and L. Kanz. 1996. Developmental regulation of myeloid gene expression and demethylation during ex vivo culture of peripheral blood progenitor cells. *Blood* 87: 447–455.
23. Gordon, S., and P. R. Taylor. 2005. Monocyte and macrophage heterogeneity. *Nat. Rev. Immunol.* 5: 953–964.
24. Jenkins, S. J., D. Ruckerl, P. C. Cook, L. H. Jones, F. D. Finkelman, N. van Rooijen, A. S. MacDonald, and J. E. Allen. 2011. Local macrophage proliferation, rather than recruitment from the blood, is a signature of TH2 inflammation. *Science* 332: 1284–1288.
25. Hamerman, J. A., and A. Aderem. 2001. Functional transitions in macrophages during in vivo infection with *Mycobacterium* bovis bacillus Calmette-Guérin. *J. Immunol.* 167: 2227–2233.
26. Felix, R., M. G. Cecchini, and H. Fleisch. 1990. Macrophage colony stimulating factor restores in vivo bone resorption in the op/op osteopetrotic mouse. *Endocrinology* 127: 2592–2594.
27. Felix, R., M. G. Cecchini, W. Hofstetter, P. R. Elford, A. Stutzer, and H. Fleisch. 1990. Impairment of macrophage colony-stimulating factor production and lack of resident bone marrow macrophages in the osteopetrotic op/op mouse. *J. Bone Miner. Res.* 5: 781–789.
28. Wiktor-Jedrzejczak, W., E. Urbanowska, S. L. Aukerman, J. W. Pollard, E. R. Stanley, P. Ralph, A. A. Ansari, K. W. Sell, and M. Szperl. 1991. Correction by CSF-1 of defects in the osteopetrotic op/op mouse suggests local, developmental, and humoral requirements for this growth factor. *Exp. Hematol.* 19: 1049–1054.
29. Lagasse, E., and I. L. Weissman. 1997. Enforced expression of Bcl-2 in monocytes rescues macrophages and partially reverses osteopetrosis in op/op mice. *Cell* 89: 1021–1031.
30. MacDonald, K. P., J. S. Palmer, S. Cronau, E. Seppanen, S. Olver, N. C. Raffelt, R. Kuns, A. R. Pettit, A. Clouston, B. Wainwright, et al. 2010. An antibody against the colony-stimulating factor 1 receptor depletes the resident subset of monocytes and tissue- and tumor-associated macrophages but does not inhibit inflammation. *Blood* 116: 3955–3963.
31. Hashimoto, D., A. Chow, C. Noizat, P. Teo, M. B. Beasley, M. Leboeuf, C. D. Becker, P. See, J. Price, D. Lucas, et al. 2013. Tissue-resident macrophages self-maintain locally throughout adult life with minimal contribution from circulating monocytes. *Immunity* 38: 792–804.
32. Ginhoux, F., M. Greter, M. Leboeuf, S. Nandi, P. See, S. Gokhan, M. F. Mehler, S. J. Conway, L. G. Ng, E. R. Stanley, et al. 2010. Fate mapping analysis reveals that adult microglia derive from primitive macrophages. *Science* 330: 841–845.
33. Schulz, C., E. Gomez Perdiguero, L. Chorro, H. Szabo-Rogers, N. Cagnard, K. Kierdorf, M. Prinz, B. Wu, S. E. Jacobsen, J. W. Pollard, et al. 2012. A lineage of myeloid cells independent of Myb and hematopoietic stem cells. *Science* 336: 86–90.